

Finding the optimum activation energy in DNA breathing dynamics: a simulated annealing approach

Pinaki Chaudhury¹, Ralf Metzler² and Suman K Banik³

¹ Department of Chemistry, University of Calcutta, 92 A P C Road, Kolkata 700 009, India

² Department of Physics, Technical University of Munich, D-85747 Garching, Germany

³ Department of Chemistry, Bose Institute, 93/1 A P C Road, Kolkata 700 009, India

E-mail: pinakc@rediffmail.com, metz@ph.tum.de and skbanik@bic.boseinst.ernet.in

Received 22 April 2009, in final form 2 July 2009

Published 28 July 2009

Online at stacks.iop.org/JPhysA/42/335101

Abstract

We demonstrate how the stochastic global optimization scheme of simulated annealing can be used to evaluate optimum parameters in the problem of DNA breathing dynamics. The breathing dynamics is followed in accordance with the stochastic Gillespie scheme, the denaturation bubbles in double-stranded DNA being studied as a single molecule time series. Simulated annealing is used to find the optimum value of the activation energy for which the equilibrium bubble size distribution matches with a given value. It is demonstrated that the method overcomes even large noise in the input surrogate data.

PACS numbers: 87.15.Av, 05.40.-a, 87.14.Gg, 02.60.Pn, 87.80.Nj

1. Introduction

Optimization techniques have successfully been used across the disciplines [1–7]. In general, a given problem is cast in a manner such that finding the extremum point of a functional in some search space renders the desired solution. For illustration, consider the non-trivial problem of finding the global minimum in a rugged potential energy surface. In this problem one starts from any arbitrary point, and then moves on the search space following certain criteria (one could be that a move is accepted if the gradient norm decreases in a given move) and converges on a point for which the gradient norm is zero. To verify whether the obtained point is indeed a minimum or not, one needs to check if the eigenvalues of the associated Hessian matrix at that point are all positive or not. In general, for any problem in which a finite number of optimum values of parameters are sought after, one can write an adequate functional and extremize it by following the above procedure.

However, an optimization procedure whose mode of action is solely guided by minimizing the local gradient norm (one which is deterministic) may face difficulties, especially in search spaces with multiple minima. If the obtained minimum is a local one, there is no way

of escaping from it again and moving toward the global minimum. Here the concept of true global optimizers, whose search is not solely driven by a local gradient, or one which is generically stochastic in nature, is needed. Simulated annealing (SA) is such a global optimizer and has been very successfully used since it was originally introduced by Kirkpatrick *et al* [8]. In particular, in these references SA was used to tackle the famed traveling salesman problem (a so-called nondeterministic polynomial (NP) time problem). Due to its successful application a large amount of literature on SA has been published across fields, see, for instance, [9–13].

SA is a search technique which borrows its concepts from the physical process of annealing. If one is trying to produce a good alloy, a molten state of the metallic mixture is prepared at a very high temperature (starting annealing temperature T_{at}) and then gradually cooled. If the rate of cooling (*annealing schedule*) is slow enough the system will solidify at the minimum (stable) thermodynamic state. SA exactly follows this principle. The search space is sampled initially at a high temperature (T_{at}), and then gradually at lower values of T_{at} determined by a preassigned schedule. The temperature T_{at} controls the strength of thermal fluctuations, so that even if the system is trapped in a local minimum, a high enough T_{at} can take it out of the attractive basin and the search can carry on to locate deeper minima, and eventually the global one. In the limit of very small T_{at} or if the search is carried on for a sufficient length of time, the global minimum will be unequivocally found. Operational details of this procedure are presented below.

In this communication, we employ SA to study the dynamics of DNA denaturation bubbles. We show that SA finds the optimum value of the activation energy for base pair breaking and therefore reproduces correctly the bubble free energy landscape. Moreover we demonstrate that SA performs well even in the presence of strong noise superimposed on the surrogate input data. In the optimization procedure we start with an arbitrary value of the activation energy and allow SA to improve it until the bubble size distribution matches a given distribution. We specifically use SA in this problem as we believe it is well suited to analyze experimental data on DNA bubble dynamics.

This paper is organized as follows. In the following we first discuss the methodology of SA in detail and connect it to the optimization of the activation energy required for DNA base pair opening. Then the simulation results are presented and discussed, and finally the paper is concluded.

2. DNA bubble dynamics and simulated annealing

Double-stranded DNA can locally denature, i.e., the base pairs usually forming the double-helix break [14]. The result is a DNA bubble consisting of single-stranded DNA, see figure 1. Driven by thermal fluctuations this bubble changes its size by breaking or reannealing of base pairs at the two interfaces between bubble and intact double strand [14]. The resulting DNA breathing or DNA bubble dynamics therefore is a stochastic process [15–17]. To follow the time series of the kinetics one needs to resort to a formulation that intrinsically includes the fluctuations in an efficient way. It was shown in [16] that the Gillespie algorithm [18], in which the multi-step rate equation is written as a single master equation, provides time series and equilibrium quantities of bubble breathing dynamics.

A denaturation bubble opens (nucleates) with an initiation free energy factor $\sigma_0 = \exp(-E_s/k_B T) \approx 10^{-5} \dots 10^{-3}$ at room temperature [19]. Once initiated, additional base pairs break with a free energy $E(T)$, with associated statistical weight $u = \exp(-E(T)/k_B T)$. This free energy $E(T)$ is composed of the free energies for hydrogen bonding and base stacking [20]. In general, the value of $E(T)$ will depend on the type of nearest-neighbor base pairs (AT or GC) [20]; however, here we consider a homopolymer DNA in which all $E(T)$ are

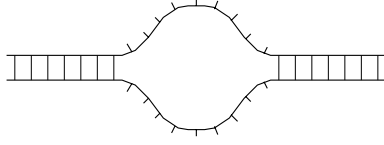


Figure 1. DNA denaturation bubble. The bubble consists of single-stranded DNA that is embedded in a still intact double strand. At the interface between bubble and double strand, base pairs break or reanneal stochastically, giving rise to the bubble dynamics.

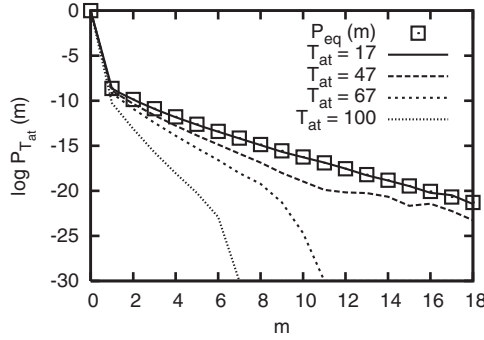


Figure 2. Plot of the equilibrium probability $P_{eq}(m)$ to find a bubble of m broken base pairs for a bubble domain of maximum size $m = 18$. The parameters for the open boxes are $\sigma_0 = 10^{-3}$ and $u = 0.6$. We also show the SA estimates $P_{T_{at}}(m)$ at various annealing temperatures T_{at} . The plot for $T_{at} = 17$ matches quite well with the preset surrogate equilibrium distribution, $P_{eq}(m)$.

equal. Thermal melting of the DNA double strand defining the melting temperature T_m occurs when $E(T_m) = 0$. Below the melting temperature the fully closed (no bubble) state will always be favorable. However fluctuations may initiate a transient bubble. The ensuing opening/closing dynamics of a single DNA bubble can in fact be monitored in fluorescence correlation experiments [21]. At equilibrium the probability distribution to find a bubble of size m broken base pairs is plotted in figure 2 with logarithmic ordinate. The initial jump corresponds to the initiation free energy factor σ_0 . Subsequently one observes a straight decay corresponding to the investment of the free energy $E(T)$ per broken base pair.

In this work we wish to employ a stochastic optimization search for the correct determination of u at the particular temperature in which the system is studied. For this we have a theoretical probability distribution profile for the occupation at various DNA sites [16] with which we will compare our distribution profiles for various u values determined for different annealing temperatures given by the annealing protocol. SA will guide our search for the optimum u such that we arrive at the theoretical distribution profile in as few iterations as possible.

In the SA algorithm thermal fluctuations are used to cross barriers in the underlying search landscape such that optimum parameters can be found even in a rugged surface. The simulation is started at a sufficiently high annealing temperature T_{at} . This makes nearly all moves acceptable as the criterion for accepting or rejecting a move is determined by the Metropolis criterion. In our case the objective function (often called *cost function* in the SA language) which is being minimized is the sum of the squares of the difference of the occupation probabilities at the various sites

$$\text{cost} = \sum_{i=1}^m (P_{eq}(m) - P_{T_{at}}(m))^2, \tag{1}$$

where $P_{\text{eq}}(m)$ denotes the preset surrogate probability distribution to have m broken base pairs, and $P_{T_{\text{at}}}(m)$ is the distribution obtained from SA at temperature T_{at} . If, on going from one step to the other in the annealing protocol defined below, the magnitude of the cost function decreases, this move is accepted. If it increases, the move is not discarded immediately. We subject it to the Metropolis test [22]: the quantity

$$\Delta = \text{cost}_i - \text{cost}_{i-1} \quad (2)$$

is computed where cost_i is the magnitude of the cost in the present step and cost_{i-1} is the value at the step before. As we observe an increase in the cost function, the quantity Δ is positive. The probability of accepting this move is then determined by evaluating the function

$$F = \exp(-\Delta/T_{\text{at}}). \quad (3)$$

By definition F ranges between 0 and 1. For each evaluation of F we invoke a random number Rn between 0 and 1. If F is greater than Rn we accept the move, following the idea that the cost increase corresponding to the 'Boltzmann factor' F is smaller than the intensity of the fluctuation corresponding to the random number Rn . If $F < Rn$ the move is rejected. Thus at high T_{at} , F will be close to 1 and most moves will be accepted, and a greater region of search space will be sampled. As the simulation proceeds, T_{at} is lowered by following the annealing schedule, as the optimization proceeds. This decrease in T_{at} can be a simple decrease by a certain factor or an exponential decrease depending on the nature of the problem. Once on the right path toward the global minimum we need not search the entire space and concentrate on a small region which will funnel the search specifically to the global minimum. As T_{at} is lowered less and less moves pass the Metropolis test. More and more of the accepted moves correspond to a decrease in the cost function and we move toward the global minimum. In the current setup it is the value of the base pair breaking free energy factor u for which F is minimized.

3. Results and discussion

We focus on the evolution of a few quantities important to characterize the denaturation bubbles, as we move through the annealing schedule. The optimum search for u was started with the cost function far away from zero, the starting value being close to 0.1; the starting guess value of u chosen here is arbitrary, which could easily have been some other value far from the actual solution. In our simulation the annealing schedule was a 2% decrease in T_{at} , i.e., starting with an initial annealing temperature of $T_{\text{at}} = 100$ after each simulation step (or temperature step) T_{at} was decreased by 2% of its current value. For each temperature step T_{at} in the SA run, a maximum of 30 samplings were carried out, however, in cases when 20 steps were successful from the Metropolis sampling, the simulation was started at the next lower annealing temperature obtained following the annealing schedule. In figure 3 we plot the profile of u against the inverse of the annealing temperature T_{at} . The convergence is rapid toward the correct value $u = 0.6$, reaching $u = 0.5997$ after about 10 iterations. The simulation is carried on for more steps to ensure that the obtained value corresponds to a final plateau.

During sampling for moves which pass the Metropolis test, the instantaneous values of u can show fluctuations at a particular annealing temperature (as one samples the system a number of times at a given annealing temperature) and more so when the annealing temperature is high. This fluctuations in u will decrease as we move closer to the solution which is achieved at a lower annealing temperature. This is because the Metropolis sampling scheme is such that a smaller and smaller number of moves is accepted as the annealing temperature goes on

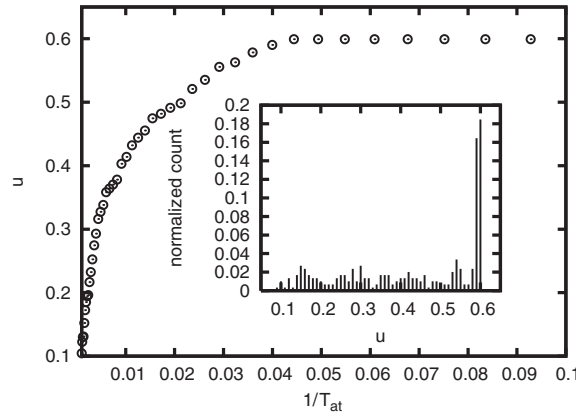


Figure 3. Plot of the SA estimate of the statistical weight factor u versus the annealing temperature $1/T_{at}$. Inset: histogram showing the Metropolis sampling of instantaneous fluctuations in u for the entire range of annealing temperature performed during the optimization process. The main figure plots the best u at a given temperature step obtained from the fluctuating data shown in the histogram.

decreasing. The histogram in the inset of figure 3 depicts this fluctuations in u for the entire range of annealing temperature in the SA sampling performed. Initially, the u values show higher fluctuations as these correspond to sampling at a higher annealing temperature, but these fluctuations gradually decrease and near the vicinity of the solution u values other than those close to the actual solution are not accepted. Hence, the maximum normalized count in the inset of figure 3 corresponds to $u = 0.6$, which is the actual solution.

In figure 2 we plot the evolution of the bubble size distribution $P_{T_{at}}(m)$ for some different annealing temperatures T_{at} . It can be seen that at higher T_{at} finer details of the population of the free energy landscape, corresponding to the occupation of large bubble states (high m), are not sampled, and consequently the probability distribution falls off too quickly. At successively lower temperatures the profile found from SA converges toward the true equilibrium distribution of the bubble. While the curve for $T_{at} = 100$ is far away from the equilibrium data, the curve for $T_{at} = 17$ exactly superimposes on the equilibrium profile. The other two curves for $T_{at} = 67$ and $T_{at} = 47$ show the intermediate dynamics and approach toward the equilibrium profile, respectively. This is done so that we can follow the subtle features of the dynamics and exactly track whether larger m th sites get populated or not. The observation is that as we proceed a significant population develops at larger m values with the decay from higher m to lower m becoming more gradual. This is expected physically since rare events need a finer sampling resolution (note the logarithmic axis in figure 2).

To test the robustness of the SA procedure, we also carried out calculations to see how a very noisy distribution profile, created by introducing reasonable perturbations onto the equilibrium distribution data ($P_{eq}(m) \pm \lambda \times rn$, $\lambda \sim 5$, $rn \in [0, 1]$), converges to the correct one. The results of the calculation are shown in figure 4. The SA run was started with the zigzag profile (solid line) denoted as noisy data. The starting temperature was kept pretty large (at nearly 10^6), since the cost function was of a large value to start with. In this case the cost function can be written as

$$\text{cost}_{(u=0.6)} = \sum_{i=1}^m (P_{eq}(m) - P_{T_{at}}(m))^2, \quad (4)$$

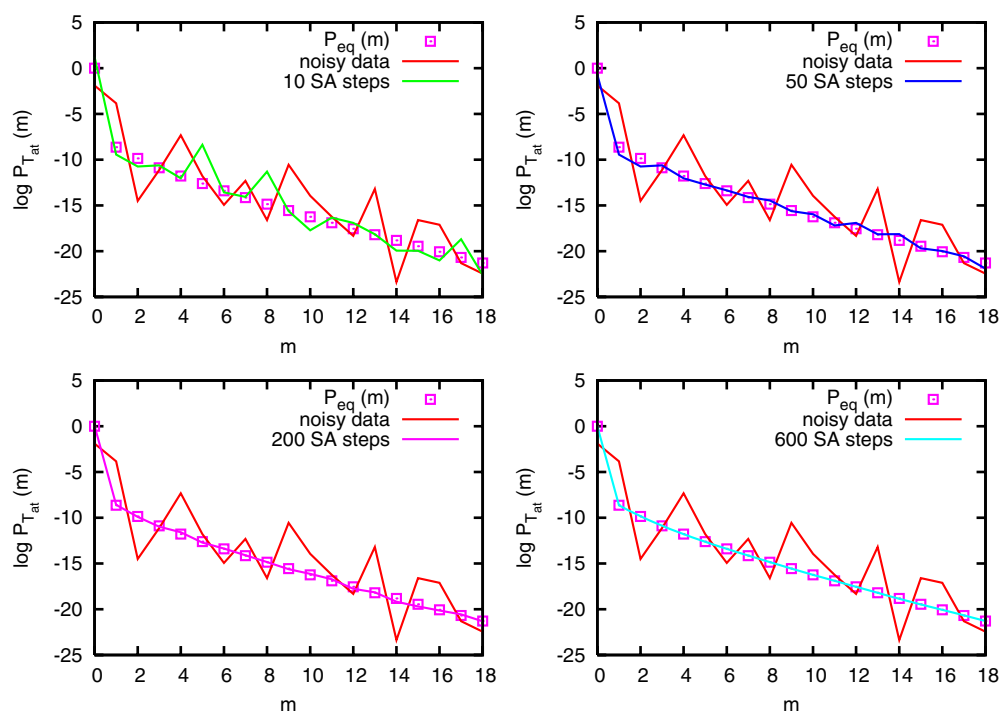


Figure 4. Plot of $\log P_{T_{at}}(m)$ against m at various SA steps. The plot for 600 steps matches the theoretical distribution.

(This figure is in colour only in the electronic version)

which looks similar to equation (1), with the only interpretational change being that we are trying to find out the correct distribution, keeping the activation energy $u = 0.6$ in all the cases. The goal of the SA run is to smoothen the noisy profile and reach the optimum distribution (given by symbols) for $u = 0.6$. Gradually with the progress of the calculation at successive steps (10, 50, 200 and 600) the profile becomes more regular, with the noisy structures vanishing and at the 600 th step a profile which matches the exact theoretical one is generated as is evident from figure 4.

4. Conclusion

Potential application of the SA algorithm presented in this work will analyze experimental single molecule data. Currently, except in one case, there are no available experimental data. The only experimental data that are available come from fluorescence correlation measurement [21]. However, it is only a question of time until new experimental data become available. Considering this the present communication tries to establish a groundwork which can be further extended to analyze experimental data in the future.

Another potential application of SA would be the subject of recent publication [23] in which a novel setup for obtaining more accurate data for DNA denaturation has been proposed. In particular, this setup has the potential to reveal position-resolved data. Having these potential experiments in mind we wanted to find out the potential of SA to actually tackle the involved analysis. In the submitted work we show that this is actually possible.

As we show in the present work, the SA algorithm is extremely insensitive to noisy input data; even after adding random values of significant amplitude to the input data the correct parameters are found. This was not necessarily expected *a priori*, and this is what we consider a major result of our work.

In this work we have shown how optimum parameters in systems of biological interest can be found out with the use of stochastic optimization techniques. These results have inspired us to look into more complicated problems, like a two-dimensional model in which not only the size of the bubble but the exact position of cleavage of base pairs can be found out [17]. In addition to that, the experimental work involving single molecule techniques so far concentrates on homopolymer DNA. It will be interesting to see what power SA exhibits when longer and heteropolymer structures are tested. Work in this direction is in progress, which we wish to address in our future communications.

Acknowledgments

PC wishes to thank The Centre for Research on Nano Science and Nano Technology, University of Calcutta for a research grant [Conv/002/Nano RAC (2008)]. SKB acknowledges support from the Bose Institute through a initial start up fund.

References

- [1] Fogarsi G and Pulay P 1984 *Ann. Rev. Phys. Chem.* **35** 191
- [2] Pulay P and Simons J (eds) 1986 *Geometrical Derivatives of Energy Surfaces and Molecular Properties* (Dordrecht: Reidel)
- [3] Schlegel H B 1987 *Adv. Chem. Phys.* **67** 249
- [4] Head J D, Weiner B and Zerner M C 1988 *Int. J. Quantum Chem.* **33** 177
- [5] Prentiss M C, Wales D J and Wolynes P G 2008 *J. Chem. Phys.* **128** 225106
- [6] Bacelo D E and Fioressi S E 2003 *J. Chem. Phys.* **119** 11695
- [7] Liu P and Berne B J 2003 *J. Chem. Phys.* **118** 2999
- [8] Kirkpatrick K S, Gelatt C D and Vecchi M P 1983 *Science* **220** 671
Kirkpatrick K S 1984 *J. Stat. Phys.* **34** 975
- [9] Car R and Parinello M 1985 *Phys. Rev. Lett.* **55** 2471
- [10] Nandy S, Chaudhury P, Sharma R and Bhattacharyya S P 2008 *J. Theor. Comput. Chem.* **7** 777
- [11] Dutta P, Mazumdar D and Bhattacharyya S P 1991 *Chem. Phys. Lett.* **181** 288
- [12] Mingjun J and Huanwen T 2004 *Chaos Solitons Fractals* **21** 933
- [13] Lyman E and Zuckerman D M 2007 *J. Chem. Phys.* **127** 065101
- [14] Poland D and Scheraga H A 1970 *Theory of Helix-Coil Transitions in Biopolymers* (New York: Academic)
- [15] Hanke A and Metzler R 2003 *J. Phys. A: Math. Gen.* **36** L473
Fogedby H C and Metzler R 2007 *Phys. Rev. Lett.* **98** 070601
- [16] Banik S K, Ambjörnsson T and Metzler R 2005 *Europhys. Lett.* **71** 852
- [17] Ambjörnsson T, Banik S K, Krichevsky O and Metzler R 2006 *Phys. Rev. Lett.* **97** 128105
Ambjörnsson T, Banik S K, Krichevsky O and Metzler R 2007 *Biophys. J.* **92** 2674
- [18] Gillespie D T 1976 *J. Comput. Phys.* **22** 403
Gillespie D T 1977 *J. Phys. Chem.* **81** 2340
- [19] Blake R D, Bizzaro J W, Blake J D, Day G R, Delcourt S G, Knowles J, Marx K A and SantaLucia J Jr 1999 *Bioinformatics* **15** 370
- [20] Krueger A, Protozanova E and Frank-Kamenetskii M D 2006 *Biophys. J.* **90** 3091
- [21] Altan-Bonnet G, Libchaber A and Krichevsky O 2003 *Phys. Rev. Lett.* **90** 138101
- [22] Metropolis N, Rosenbluth A W, Rosenbluth M N, Teller A H and Teller E 1953 *J. Chem. Phys.* **21** 1087
- [23] Pedersen J N, Hansen M S, Novotný T, Ambjörnsson T and Metzler R 2009 *J. Chem. Phys.* **130** 164117
Novotný T, Pedersen J N, Hansen M S, Ambjörnsson T and Metzler R 2007 *Europhys. Lett.* **77** 48001